Available online at www.sciencedirect.com
SCIENCE DIRECT
Spectrochimica Acta Part A 62 (2005) 353–363
SPECTROCHIMICA ACTA PART A
www.elsevier.com/locate/saa

Conformational analysis and crystal structure of {[1-(3-chloro-4-fluorobenzoyl)-4-fluoropiperidin-4yl]methyl} [(5-methylpyridin-2-yl)methyl]amine, fumaric acid salt

J.P. Ribet [a,*], R. Pena [a], J.L. Maurel [a], C. Belin [b], M. Tillard [b], B. Vacher [a], B. Bonnaud [a], F. Colpaert [a]

[a] *Institut de Recherche Pierre Fabre, 17 avenue Jean Moulin, 81106 Castres, France*
[b] *Laboratoire des Agrégats Moléculaires et Matériaux Inorganiques, UMR 5072 CC15, Université de Montpellier II, Sciences et Techniques du Languedoc, 2 Place Eugène Bataillon, 34095 Montpellier Cédex 5, France*

Received 15 November 2004; accepted 12 January 2005

Abstract

{[1-(3-Chloro-4-fluorobenzoyl)-4-fluoropiperidin-4yl]methyl}[(5-methylpyridin-2-yl)methyl]amine, fumaric acid salt ($C_{20}H_{22}ClF_2N_3O$, $C_4H_4O_4$) (**1**) was synthesized and characterized by the complete ^1H, ^{13}C and ^{19}F NMR analyses. The conformation of the piperidin ring, in the solution state, was particularly studied from the coupling constants determined by recording a double-quantum filtered COSY experiment in phase-sensitive mode. ^1H NMR line-shape analysis was used, at temperatures varying between −5 and +60 °C, to determine the enthalpy of activation of the rotational barrier around the C–N bond. Compound **1** crystallizes in the triclinic space group $P\bar{1}$ with $a = 8.517(3)$ Å, $b = 12.384(2)$ Å, $c = 12.472(3)$ Å, $\alpha = 70.88(2)^\circ$, $\beta = 82.04(2)^\circ$, $\gamma = 83.58(2)^\circ$.

The results strongly indicate that the solid and solution conformations are similar. Thermal stability and phases transitions were investigated by thermal gravimetric analysis (TGA) and differential scanning calorimetry (DSC). Furthermore polymorphism screening was studied from recrystallization of **1** performed in seven solvents and by slurry conversion in water. The X-ray powder diffraction (XRPD) and differential scanning calorimetry results suggested that **1** crystallizes into one crystalline form which melts at 157 °C ($\Delta H = 132\ J\ g^{-1}$).

Keywords: Conformational analysis; Crystal structure; Thermal analysis; Polymorphism study; 5-HT_{1A} receptor agonist

1. Introduction

The present study was undertaken to determine the conformation in solution and the structure in the solid state of {[1-(3-chloro-4-fluorobenzoyl)-4-fluoropiperidin-4yl]methyl}[(5-methylpyridin-2-yl)methyl]amine, fumaric acid salt ($C_{20}H_{22}ClF_2N_3O$, $C_4H_4O_4$; **1**, Fig. 1) a novel 5-HT_{1A} receptor agonist. This molecule is characterized by a high affinity for 5-HT_{1A} receptors and a high selectivity versus α1 and D_2 [1,2]. The 5-HT_{1A} subtype of serotonin (5-HT) receptors are implicated in many psychiatric and neurological disorders [3,4]. NMR studies are performed to help the understanding of the relationship between the conformation of the pharmacophore in the solution state and the agonist activity at 5-HT_{1A} receptors. Dynamic aspects are studied by two-dimensional spectrometry (NOESY) because the conformation of the amide bond is an important subject, not only in pure chemistry but also in medicinal chemistry. Rate constants for the rotational barrier are measured over a range of temperatures using ^1H NMR line-shape analysis from which the enthalpy of activation is obtained. These observations provide evidence of the usefulness of NMR spectrometry to establish the active conformation of the ligand. Furthermore, the restricted rotation around the C–N bond in solution could explain the appearance of conformational polymorphism in the solid state. Polymorphism is the ability for a compound to exist in more than one crystal form

* Corresponding author. Tel.: +33 5 63 71 42 79; fax: +33 5 63 71 42 99.
E-mail address: jean.paul.ribet@pierre-fabre.com (J.P. Ribet).

1386-1425/$ – see front matter © 2005 Elsevier B.V. All rights reserved.
doi:10.1016/j.saa.2005.01.002

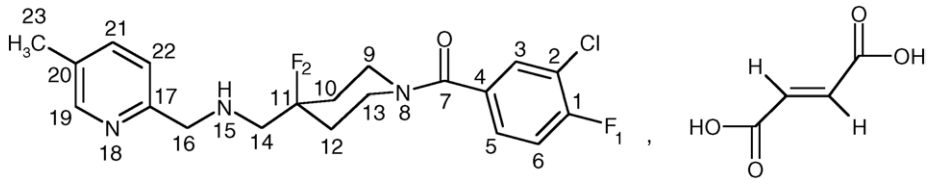

Fig. 1. Structural formula of **1** the {[1-(3-chloro-4-fluorobenzoyl)-4-fluoropiperidin-4yl]methyl}[(5-methylpyridin-2-yl)methyl]amine, fumaric acid salt.

with different unit cell parameters and conformational polymorphism occurs when different conformational isomers of a compound crystallize as distinct polymorphs. Differences in solubility between crystal forms can lead to difference in bio-availability of solid dosage forms if the bio-availability is dissolution limited. Thus, a polymorph screening is performed by crystallization and slurry processes in various solvents. The solid state property of the samples is studied by differential scanning calorimetry (DSC), thermal gravimetric analysis (TGA) and X-ray powder diffraction (XRPD). The data presented herein, indicate that **1** exists in only one crystal form. The structure of this polymorphic form is determined with the help of crystallographic data.

2. Experimental

2.1. Synthesis

In a previous technique, illustrated by WO 98/22459 [5] the title compound was obtained in nine steps. First, the 3-chloro-4-fluoro-benzoylchloride was obtained starting from the corresponding benzoic acid and thionyl chloride, and was condensed with 4,4-ethylenedioxy-piperidine to give 8-(3-chloro-4-fluorobenzoyl)-1,4-dioxa-8-azaspiro[4,5]decane. Then, the 1-(3-chloro-4-fluorobenzoyl)piperidin-4-one was obtained in acidic media, and a Darzens condensation was carried out to give 6-(3-chloro-4-fluorobenzoyl)-2-cyano-1-oxa-6-azaspiro[2.5]octane which was opened with hydrofluoric acid–pyridine complex to a cyanohydrine: [1-(chloro-4-fluorobenzoyl)-4-fluoropiperidin-4-yl](cyano)methanol. This cyanohydrine intermediate was the starting material of our new reaction. Previously, this cyanohydrine was transformed in [1-(chloro-4-fluorobenzoyl)-4-fluoropiperidin-4-yl]methanol by reduction with sodium borohydride, and then, activated with paratoluene sulfonyl chloride, condensed on potassium phtalimide to give the {[1-(chloro-4-fluorobenzoyl)-4-fluoropiperidin-4-yl]methyl}amine, after opening the phtalimide by ethanolamine. This {[1-(chloro-4-fluorobenzoyl)-4-fluoropiperidin-4-yl]methyl}amine was condensed on 5-methylpyridine-2-carbaldehyde to afford, after sodium borohydride reduction, the desired compound. The global yield, starting from the cyanohydrine was about 20%, calculated on a 2.5 kg size batch. A new one-pot reaction replaces favorably this succession of five steps synthesis (FR 2820743–A1) [6]. The cyanohydrine was directly stirred with [(5-methylpyridin-2-yl)methyl]amine in basic and reductive media in methanol. This, was obtained using a mixture of 1,4-diazabicyclo[2,2,2]octane (DABCO) and sodium cyanoborohydride. This process gave directly the {[1-(3-chloro-4-fluorobenzoyl)-4-fluoropiperidin-4yl]methyl}[(5-methylpyridin-2-yl)methyl]amine with a 87% yield. This oil was treated in ethyl acetate with fumaric acid alcoholic solution to give a crystalline salt. The stoichiometry of the salt was 1/1 molar and the molecular weight was 509.95 g mol^{-1}. Chemical purity of sample was superior to 99.5% (w/w) evaluated by HPLC and internal normalization.

2.2. Nuclear magnetic resonance spectrometry (NMR)

All spectra were recorded non-spinning on a Bruker Avance 400 spectrometer operating at the proton nominal frequency of 400 MHz equipped with a 5 mm inverse multinuclear gradient probe-head. The spectrometer frequency was 400.13 MHz for ^{1}H. Variable-temperature experiments were made using the BVT 3300 and the BCU-05 accessories of the instrument. Temperature probe was calibrated by studying the temperature dependence in the chemical shifts of the methylene and hydroxyl resonances in an 80% ethylene glycol–20% dimethylsulfoxide sample tube (Bruker Ref Z10129, 7493 A). The confidence interval was $\pm 1\,^{\circ}$C.

For the structural analysis by ^{1}H NMR and ^{13}C NMR the compound was dissolved in dimethylsulfoxide-d_6 (Eurisotop D310-B, batch Q 2801) at approximately 17 mM concentration and the temperature of the probe was maintained to 25 °C. The chemical exchange was studied by analysis of the line shapes at temperatures varying between −5 and +60 °C in methyl alcohol-d_4 (isotopic enrichment 99.80%, Eurisotop D324-B, batch L2831) with 0.03% of tetramethylsilane used as internal standard. The chemical shifts, coupling constants and line widths of the resonances were measured at low temperatures before dynamic broadening. The measurements were carried out for solution of the title compound having concentration of ca. 14 mM. The line-shape analysis of the ^{1}H NMR spectra and the simulation of the fluorine-2 splitting pattern were performed by means of a computer program WINDNMR, Version 7.1.6, 2002 [7]. To optimize the experimental conditions of the NOESY and of the GDQF-COSY experiments, the sample was dissolved in D_2O (Eurisotop, D-214 EP, batch IO 481) at approximately 20 mM concentration. For these experiments the solution was carefully filtered through an external filter tip (45 μm, Polylabo 91943)

in a dry 5 mm sample tube (New Era Enterprises NE-HP5-9") then the solution was subjected to five freeze–pump–thraw cycles before being sealed under nitrogen. Chemical shifts δ are given in parts per million (ppm) relative to T.S.P. ((3-trimethylsilyl)-propionic acid-d_4 sodium salt) obtained from Merck (Art. 8652) used as internal standard and the coupling constants in Hz. NOESY studies were acquired in the phase-sensitive mode, using the noesytp program with a mixing time set to 400 ms and 32 scans per time increment.

The double-quantum filtered GDQF-COSY experiment was acquired in the phase-sensitive mode using time-proportional phase increment (TPPI) with a spectral width of 903.18 Hz in both dimensions (cosygpmftp program), 1 × 2K data points before and 2K × 2K after zero-filling, resulting in a digital resolution of 0.44 Hz per point in the ω_1 and ω_2 dimensions. Processing was carried out using sine-bell squared functions shifted by $\pi/2$.

^{19}F NMR spectra were recorded on the title compound at 188.2 MHz on a Bruker AC200 spectrometer, at ambient temperature, in methyl alcohol-d_4 (Euriso-top, D324 B, batch IO491) solution. Proton-decoupled and proton-coupled spectra were recorded. Chemical shifts δ are given in parts per million (ppm) relative to trifluoro-acetic acid in benzene-d_6.

2.3. X-ray diffraction

The crystallized compound was obtained as follows: 1 g of **1** was dissolved in warm isopropanol (40 mL) and allowed to stand, in an open flask, at room temperature for 8 days. The resulting crystals were filtered and dried under reduced pressure. Enraf-Nonius CAD-4 diffractometer was used for X-ray diffraction data collection at $T = 293$ K using graphite monochromated Mo Kα radiation, $\lambda = 0.71069$ Å and ω–θ scans. Three standard reflections were checked every 100 reflections without any intensity decay. Cell parameters were refined from 25 automatically centered reflections $\theta = 7.6$–$11.82°$. A total of 3195 reflections were measured up to $\theta_{max} = 25°$ within the four octants hkl, $\bar{h}kl$, $h\bar{k}l$, $hk\bar{l}$. The structure was solved by direct methods using the program SHELXS97 [8] and refinement was carried out using SHELXL97 [9]. The absorption effects ($\mu = 0.21$ mm^{-1}, transmission factors varying from 0.92 to 0.99) were corrected using the numerical procedure provided by SHELX-76 program [10]. Intensities of equivalent reflections were merged ($R_{int} = 0.0336$) into 3005 (from which 1635 with $I > 2\sigma(I)$) independent reflections used for refinements. The final refinement was carried out to $R = 0.0504$, $\omega R(F^2) = 0.1509$, weighting scheme $\omega = 1/[\sigma 2(F_0^2) + (0.0706P)^2]$ where $P = (F_0^2 + 2F_c^2)/3$, $S = 1.00$. Extinction coefficient was refined to 0.006(2). Hydrogen atoms attached to carbon are treated as riding, following the SHELXL97 HFIX/AFIX instructions; they were given an isotropic displacement parameter equal to 1.2 times the U_{eq} of the parent C atom. The hydrogen atoms attached to nitrogen and oxygen were positioned from a Fourier difference map, and both their positions and isotropic thermal displacement were refined. Electron density residuals in the final Fourier difference map were +0.49 and −0.28 e Å^{-3}. The ellipsoid plot was drawn using ORTEP-3 for windows [11] which is a MS-windows version of the current release of ORTEP-III. All computations were carried out on a Pentium 4 computer.

The powder diffraction measurements were undertaken using a Philips analytical Xpert X-ray diffractometer equipped with a copper tube, a hybrid monochromator (a parabolic multilayer mirror and a two-crystal monochromator) and the Xcelerator detector. Rietveld analyses were performed using the program LHPM-Rietica [12].

2.4. Differential scanning calorimetry

Differential scanning calorimetry was performed with a DSC Q100 (TA Instrument) equipped with Universal Analysis 2000 software. The calibration (temperature and cell constant) was done using an indium standard (SPIN, ref. LGC2601). Assays were performed at rate of 5 °C min^{-1} from 0 to 170 °C in hermetic aluminium pans (TA instruments, pan: 900793.901, lid: 900794.901) under nitrogen purge at 50 mL min^{-1}. Samples, about 5 mg, were weighed with a Sartorius ultramicrobalance MP 8.

2.5. Thermogravimetry analysis

TGA and DTG curves were obtained using a TA High Resolution 2950 thermogravimeter analyzer equipped with the Universal Analysis 2000 software (TA Instruments) and a nitrogen purge at 60 mL min^{-1}. The sample was weighed in an open aluminium crucible with a cross section area of 0.327 cm^2 and deposited in a platinum pan. The sample size was about 5–9 mg in order to cover the whole of the crucible section uniformly. The thermobalance was calibrated for temperature with the melting of tin. The magnitude and linearity of the balance response were checked with standard milligram masses.

The non-isothermal TGA was recorded at 5 °C min^{-1} from room temperature to 450 °C.

2.6. Polymorph screening

Recrystallization of **1** was performed in the following solvents: ethyl acetate, acetonitrile, methanol, ethanol, isopropanol, tetrahydrofuran, acetone. Sample was suspended into 5 mL solvent and was stirred in an oil bath at 60 °C. Solvent was added until dissolution. The solutions were cooled at room temperature and filtered when **1** precipitated otherwise solutions were cooled at +4 °C until crystallization (24 h). Powders were analyzed by X-ray powder diffraction and DSC.

Slurry conversion studies were realized in water. A saturate solution was prepared with 100 mg of **1** and 0.75 mL of water in vials closed with a screw stopple. The suspension was stirred 16 h at 45 °C, 150 rpm, with a New Brunswick Sci-

Table 1
^{1}H (400 MHz) and ^{13}C (100 MHz) NMR spectrum of **1**

Carbon	δ (^{13}C) (CD_3SOCD_3), 25 °C	δ (^{1}H) (CD_3SOCD_3), 25 °C	δ (^{1}H) (CD_3OD), 25 °C	δ (^{1}H) (D_2O), 25 °C
1	157.3 (d, 249.10)	–	–	–
2	119.7 (d, 17.95)	–	–	–
3	129.2	7.68 (dd, 7.20, 1.95)	7.61	7.59
4	133.8 (d, 3.95)	–	–	–
5	127.7 (d, 7.85)	7.45 (ddd, 8.60, 5.0, 1.95)	7.41	7.38
6	117.0 (d, 21.30)	7.50 (dd, 8.60, 8.60)	7.35	7.35
7	166.6	–	–	–
9 or 13	43.0	ax 3.15–2.95 (m) eq 3.50–3.30 (m)	ax 3.30–3.10 eq 3.70–3.55	ax 3.30–3.20 eq 3.75–3.65
10 or 12	32.5	ax 1.75–1.60 (m) eq 1.90–1.80 (m)	ax 1.80–1.70 eq 2.05–1.90	ax 1.85–1.70 eq 2.05–1.90
11	94.5 (d, 171.65)	–	–	–
12 or 10	31.9	ax 1.85–1.75 (m) eq 2.05–1.90 (m)	ax 1.90–1.80 eq 2.20–2.02	ax 1.90–1.80 eq 2.20–2.10
13 or 9	37.5	ax 3.30–3.20 (m) eq 4.40–4.20 (m)	ax 3.50–3.30 eq 4.60–4.40	ax 3.50–3.40 eq 4.45–4.35
14	55.0	2.85 (d, 19.75)	3.15	3.43
16	53.5	3.90 (s)	4.20	4.40
17	155.0	–	–	–
19	148.9	8.37 (dd, 1.50, 0.85)	8.43	8.45
20	131.5	–	–	–
21	137.0	7.60 (dd, 8.0, 1.50)	7.68	7.78
22	121.5	7.35 (d, 8.0)	7.37	7.44
23	17.5	2.30 (s)	2.35	2.35
═CH-fumaric acid	134.3	6.60 (s)	6.70	6.64
═CO-fumaric acid	166.5	–	–	–

Chemical shifts (δ, ppm) and coupling constants (J, Hz in parentheses).

entific stirrer. Afterwards the suspension was filtered, dried at 40 °C under vacuum and analyzed by DSC.

After crystallization and slurry conversion processes the stoichiometry of samples was checked by HPLC.

3. Results and discussion

3.1. Assignment of ^{1}H NMR spectrum

The numbering system adopted to designate the atoms of the molecule (Fig. 1) was used to facilitate the spectral assignments and did not correspond to the Organic Chemistry Nomenclature Commission of IUPAC.

Concerning the pyridin ring the signal at δ 8.37 was assigned to H-19 (H-α pyridin, Table 1). This proton exhibited two long-range couplings, the former with H-21 and the last with H-22 ($^{4}J_{19–21}$ = 1.50 Hz and $^{5}J_{19–22}$ = 0.85 Hz). The doublet of doublets at δ 7.60 was characteristic of H-21 and was in agreement with the di-substituted pyridin ring ($^{3}J_{21–22}$ = 8.0 Hz and $^{4}J_{21–19}$ = 1.50 Hz). Thus, the nucleus H-22 was easily assigned at δ 7.35 (d, $^{3}J_{22–21}$ = 8.0 Hz).

Concerning the tri-substituted phenyl ring the pseudo-triplet at δ 7.50 was due to the coupling of H-6 with H-5 and of H-6 with the fluorine nucleus F-1 ($^{3}J_{6–5}$ = 8.60 Hz and $^{3}J_{6–F1}$ = 8.60 Hz). At δ 7.45, H-5 exhibited a characteristic first order multiplet corresponding to its coupling with H-6 ($^{3}J_{5–6}$ = 8.60 Hz), H-3 ($^{4}J_{5–3}$ = 1.95 Hz) and the fluorine nucleus F-1 ($^{4}J_{5–F1}$ = 5.0 Hz). Finally H-3 showed a doublet of doublets at δ 7.68 ($^{4}J_{3–5}$ = 1.95 Hz, $^{4}J_{3–F1}$ = 7.20 Hz).

The aliphatic region (between 1.5 and 4.5 ppm) showed a large doublet at δ 2.85 owing to the coupling of the two protons H-14 with the vicinal fluorine nucleus F-2 ($^{3}J_{14–F2}$ = 19.75 Hz). The H-16 protons appeared downfield (δ 3.90) as singlet. The piperidin ring nuclei H-9_{eq} and H-13_{eq} were strongly deshielded comparatively to H-9_{ax} and H-13_{ax} due to the magnetic anisotropic effect of the carbonyl group. The nuclei H-9_{eq} ($\delta \approx 3.4$) and H-13_{eq} ($\delta \approx 4.3$) were in different chemical environments and therefore they had different resonance frequencies. Consequently the protons H-9_{ax} and H-13_{ax} were assigned at $\delta \approx 3.0$ and $\delta \approx 3.3$. It was known that for piperidin derivatives with a sterically fixed chair conformation, chemical differences of 0.10–1.0 ppm between the axial and equatorial nuclei were found, the axial nuclei being more strongly shielded than the equatorial. However the signal multiplicity of the protons $H_{10–12ax}$ and $H_{10–12eq}$ was not resolved from the ^{1}D NMR spectrum owing to the superposition of their resonances. This problem was outlined by performing a double-quantum filtered COSY in phase-sensitive mode (Fig. 2). Finally the secondary amine and carboxylic acid protons showed a broad resonance signal between δ 10.0 and 9.50. The phase-sensitive COSY with a double-quantum

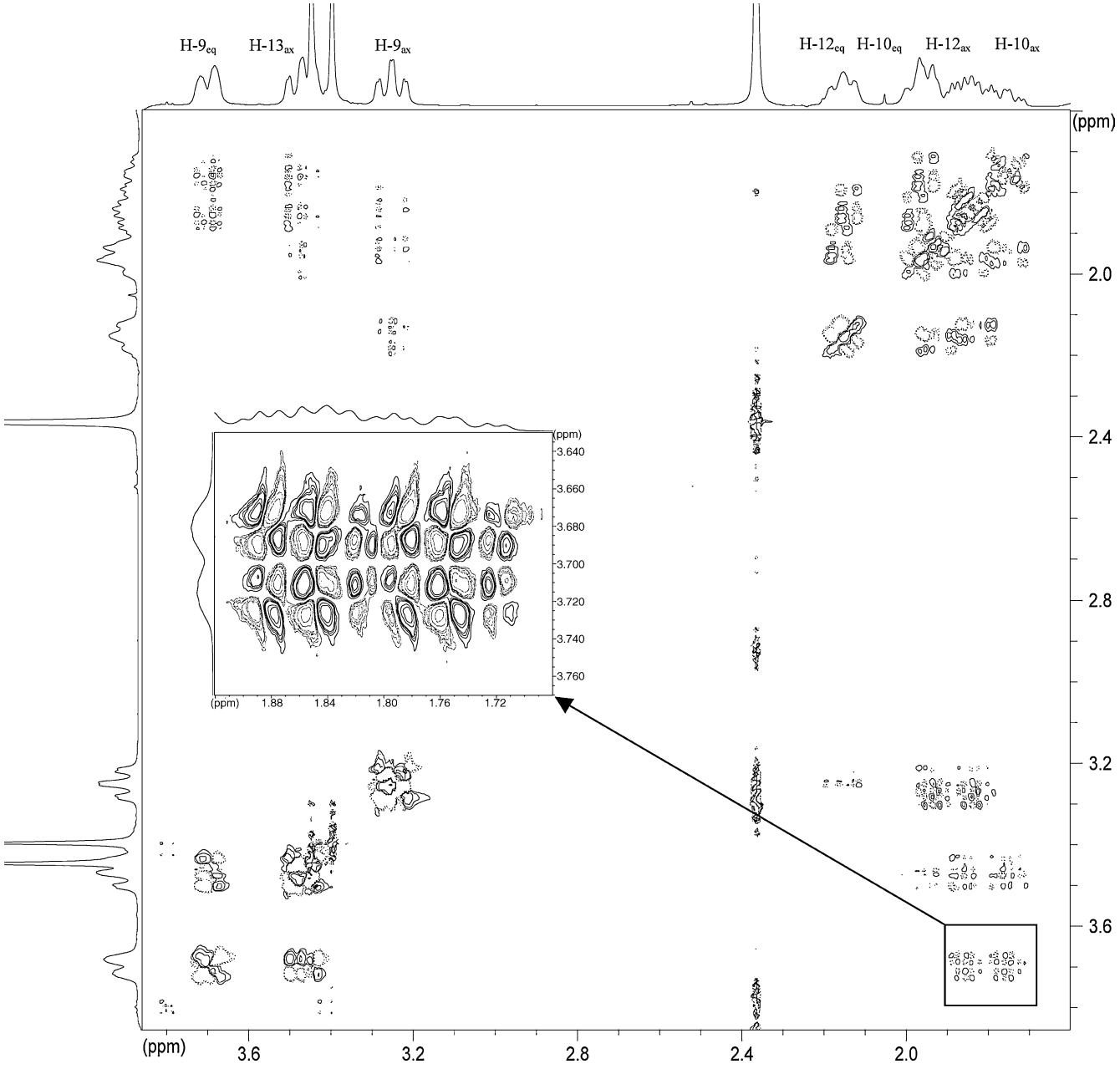

Fig. 2. Double-quantum filtered H,H-COSY spectrum of **1** in D_2O. The cross-peaks are pure antiphase, negative cross-peaks are represented by dashed contours. Spectral width in F_2 and F_1 = 903.18 Hz. The region of interest shows the multiplet structure of the cross-peak between H-10_{ax} and H-9_{eq}.

filter was the method of choice for assigning the coupling network in the 1.50–4.0 ppm region. The correlation peaks observed in pure absorption phase provided detail coupling information. The axial orientation for the fluorine F-2 was corroborated by its coupling constant with H-10_{ax} and H-12_{ax} (^3J = 36.50 Hz). This large value reflected an antiperiplanar disposition between the fluorine atom and the axial protons. In addition the coupling constant of fluorine with the equatorial protons was found equal to 10.50 Hz. These observations confirmed the rigid chair conformation of the piperidin ring and the axial orientation of the fluorine-2. If the fluorine nucleus was equatorial the coupling constant ^3JF$_2$-H$_{10ax}$ and ^3JF$_2$-H$_{10eq}$ would be inferior to 8 Hz [13]. From the expanded multiplet shown in Fig. 2 the geminal coupling constant between H-10_{ax} and H-10_{eq} was determined equal to 13.50 Hz, the vicinal coupling constant between H-10_{ax} and H-9_{eq} was found to 5.50 Hz and finally the diaxial protons H-10_{ax} and H-9_{ax} showed a typical coupling constant of about 13.50 Hz.

3.2. Assignment of ^{13}C NMR spectrum

By using heteronuclear shift correlated experiment such as HMQC and HMBC we identified all aromatic carbons and all aliphatic carbons from the knowledge of the corresponding

^{1}H NMR chemical shifts (Table 1). The carbon C-1 at δ 157.3 exhibited a large coupling constant with the fluorine nucleus F-1 ($^1J_{C1–F1}$ = 249.10 Hz). Geminal couplings were found to be $^2J_{C2–F1}$ = 17.95 Hz and $^2J_{C6–F1}$ = 21.30 Hz. Long-range couplings through more than two bonds were also determined accurately, $^3J_{C5–F1}$ = 7.85 Hz and $^4J_{C4–F1}$ = 3.95 Hz. A value of 171.65 Hz was found for coupling between C-11 and F-2 and the geminal coupling constant between C-14 and F-2 gave ^2J = 19.75 Hz [14].

3.3. Assignment of ^{19}F NMR spectrum

The fluorine resonances were characterized by large chemical shifts. The spectrum exhibited two signals under proton noise decoupling at δ −34.9 (F-1) and δ −87.3 (F-2). These values were in good agreement with those previously reported in the literature [15].

From the splitting pattern of the signal at δ −87.3 (Fig. 3) we deduced the coupling constants through three bonds ($^3J_{F2–H12ax}$ = 36.50 Hz, $^3J_{F2–H12eq}$ = 10.50 Hz and $^3J_{F2–H14}$ = 19.75 Hz). These values confirmed the axial orientation of the fluorine-2 and the rigid chair conformation of the piperidin ring. From the coupling pattern of the signal at δ −34.9 the coupling constants between the fluorine-1 and the aromatic protons were confirmed: $^3J_{H6–F1}$ = 8.60 Hz, $^4J_{H5–F1}$ = 5.0 Hz and $^4J_{H3–F1}$ = 7.20 Hz.

3.4. Nuclear Overhauser exchange spectrometry

The phase-sensitive NOESY spectrum of **1** showed positive NOEs owing to the small correlation time of the molecule in D_2O at 25 °C ($\omega\tau_c$ < 1.12). The diagonal peaks had a negative phase and the cross-peaks due to chemically exchanging protons had a phase like diagonal [16–17]. The slice at δ 4.40 exhibited two upward signals at δ 3.25 and 3.45 representing a positive NOE between H-9$_{eq}$ or H-13$_{eq}$ and H-9$_{ax}$ or H-13$_{ax}$. Similarly the slice at δ 3.70 showed positive NOE between H-9$_{eq}$ or H-13$_{eq}$ and H-9$_{ax}$ or H-13$_{ax}$. The same observation was made between H-10$_{eq}$/H-12$_{eq}$ and H-10$_{ax}$/H-12$_{ax}$. NOE cross-peaks were also observed between H-23 and the two protons H-19 and H-21. NOE appeared between H-16, H-22 and between H-16, H-14. Cross-peaks due to chemical exchange were often more intense than those due to NOE. For example the slice at δ 3.45 exhibited a large downward cross-peak at δ 3.25 corresponding to the exchange position in the molecule of the two axial protons H-9 and H-13. These two axial protons were in different chemical environment because of the restricted rotation around the C_7–N_8 bond. Therefore, ^{1}H NMR line-shape analysis was used to determine the rotational barrier of this C–N bond.

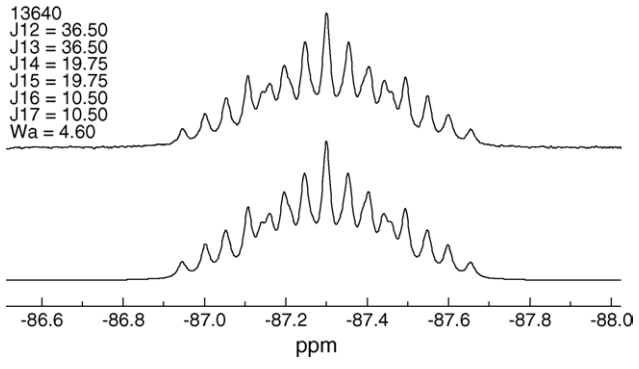

Fig. 3. Characteristic splitting pattern of the fluorine-2 at 188.2 MHz. Top, experimental and bottom, calculated ^{19}F NMR spectrum.

3.5. ^{1}H NMR line-shape analysis

C–N bond between carbonyl group and nitrogen atom has significant double bond character. At −5 °C, in methanol-d_4, the rotation around the C_7–N_8 bond was sufficiently slow on the NMR time scale to show the peaks of both H-13$_{eq}$ and H-9$_{eq}$ at respectively, δ 4.55 and 3.65 (Fig. 4). At higher temperatures the fine structure became less sharp and the chemical shift difference between H-13$_{eq}$ and H-9$_{eq}$ decreased. At +60 °C with the more rapid rotation around the C_7–N_8 bond, H-13$_{eq}$ and H-9$_{eq}$ became chemically equivalent and the lines coalesce. The enthalpy of activation for the dynamic process ($\Delta H^* = 62.0 \pm 0.9$ kJ mol^{-1}) was deduced from the slope of the Eyring plot [18,19]. At +60 °C, H-10$_{ax}$ and H-12$_{ax}$ were also chemically equivalent and appeared between δ 1.65 and 1.90 as one well resolved multiplet (Fig. 5). The multiplet splitting (≅36.50, 13.50, 13.50 and 5.50 Hz) confirmed the axial configuration of the fluorine-2 at the temperature of +60 °C. The enthalpy of activation in D_2O was found to $\Delta H^* = 83.5 \pm 1.3$ kJ mol^{-1} compared with 62.0 ± 0.9 kJ mol^{-1} in methanol. This could be attributed to stabilization of the transition state by hydrogen bonding.

3.6. Single crystal and powder X-ray study

Compound **1** crystallizes in the triclinic space group $P\bar{1}$ with cell parameters a = 8.517(3) Å, b = 12.384(2) Å, c = 12.472(3) Å, α = 70.88(2)°, β = 82.04(2)° and γ = 83.58(2)°, M = 509.93, V = 1227.8(5) Å^3, d_{cal} = 1.379 Mg m^{-3}. The unit cell contains two units of formula $C_{24}H_{26}F_2N_3O_5Cl$. The asymmetric unit is composed of one $C_{20}H_{22}F_2N_3OCl$ molecule and one fumaric acid $C_4H_4O_4$ molecule. The atomic positions and equivalent displacement parameters for atoms are reported in Table 2. Some selected structural parameters as inter-atomic distances, bond angles and torsion dihedral angles are indicated in Table 3.

The molecule $C_{20}H_{22}F_2N_3OCl$ is protonated at the nitrogen N_{15} site by a hydrogen atom from a molecule of fumaric acid. The ORTEP representation of the protonated molecule $C_{20}H_{23}F_2N_3OCl^+$ is given in Fig. 6. As expected, the aromatic chlorofluorobenzoyl cycle is flat with constituting atoms (Cl, F_1 and C_1–C_7) deviating no more than 0.035 Å from the mean atomic plane. With a deviation of 0.09 Å from the mean plane (atoms N_{18}, C_{16}, C_{17}, C_{19}–C_{23}), the methylpyridin cycle is also very flat. The atoms N_8, C_9,

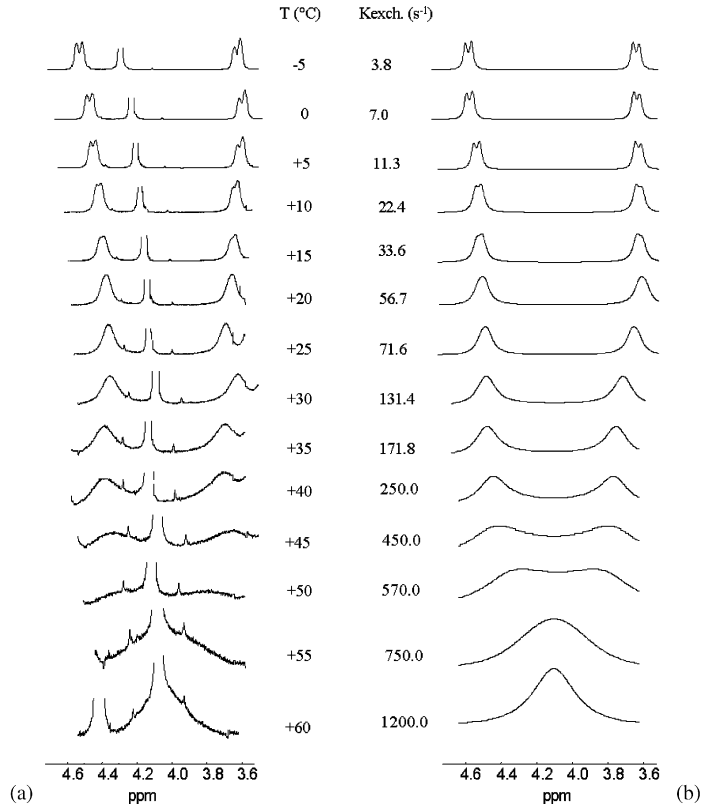

Fig. 4. Temperature dependence of the H-13_{eq} and H-9_{eq} proton resonances in methyl alcohol-d_4. The observed (a) and the calculated (b) 400.13 MHz spectrum at several temperatures.

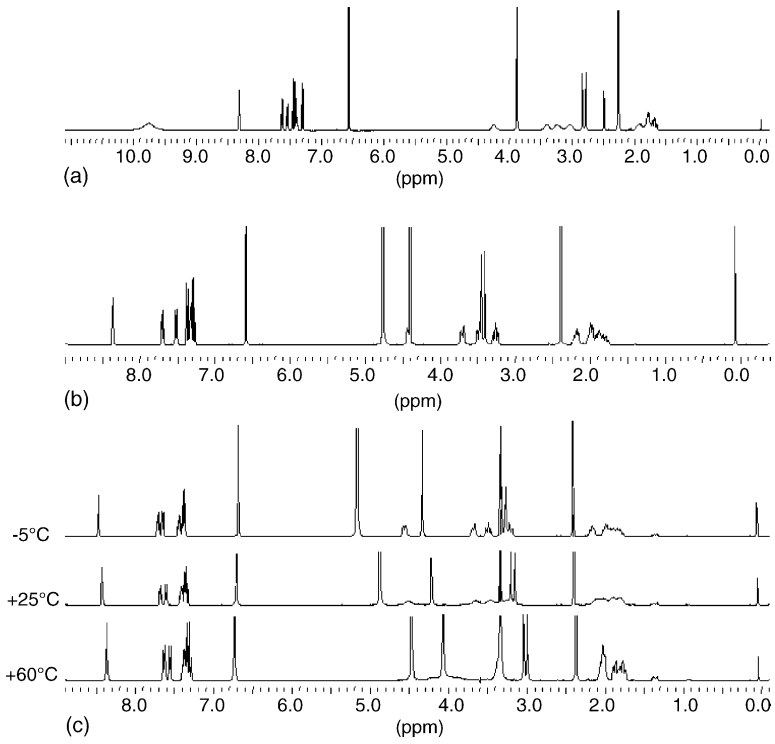

Fig. 5. ^{1}H NMR spectra of **1** (a) in DMSO-d_6 at 25 °C, (b) in D_2O at 25 °C, (c) in MeOH-d_4 at −5, +25 and +60 °C.

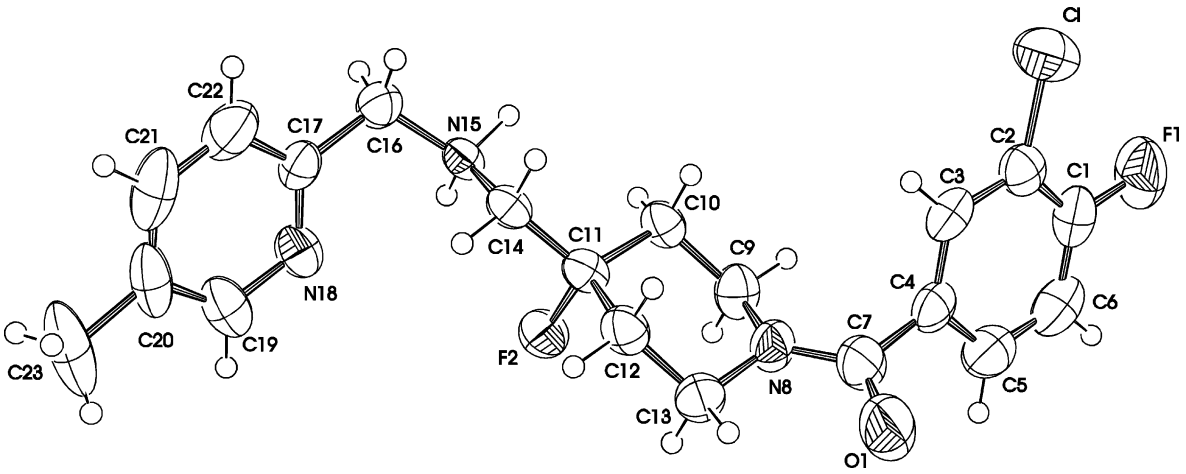

Fig. 6. ORTEP view of the {[1-(3-chloro-4-fluorobenzoyl)-4-fluoropiperidin-4yl]methyl}[(5-methylpyridin-2-yl)methyl]amine protonated molecule. Displacement ellipsoids are drawn at the 50% probability level for non-hydrogen atoms.

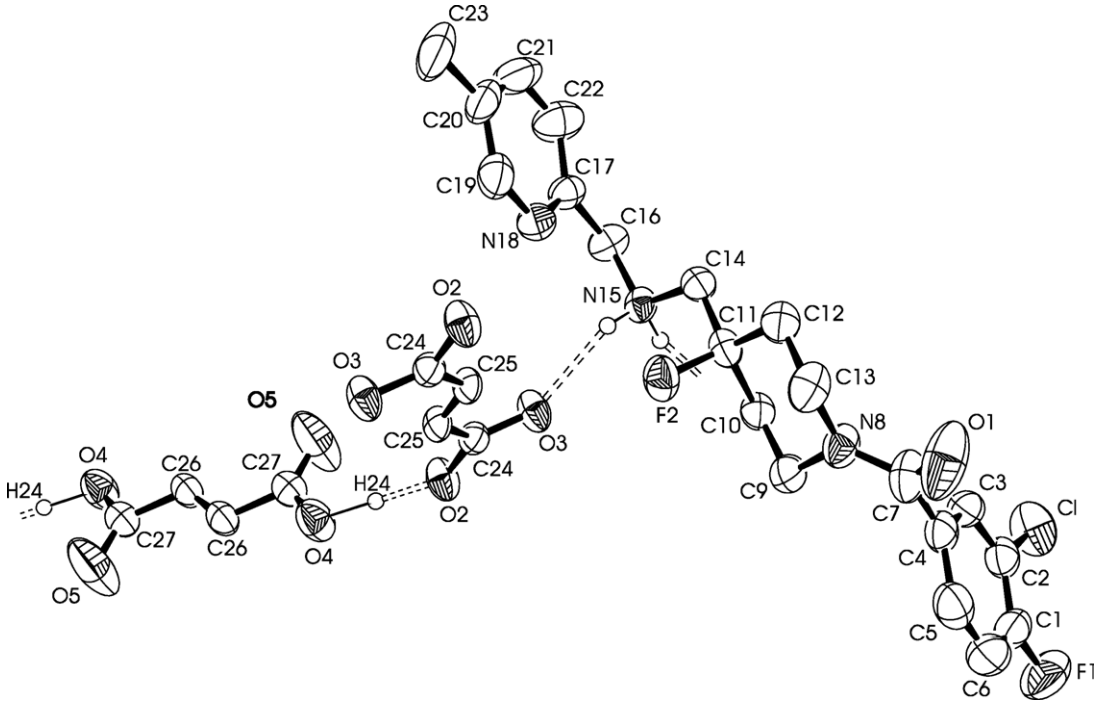

Fig. 7. Representation of the protonated molecule interacting with fumaric acid molecule via hydrogen bonding (50% probability level ellipsoids). For clarity, hydrogen atoms attached to carbon are omitted.

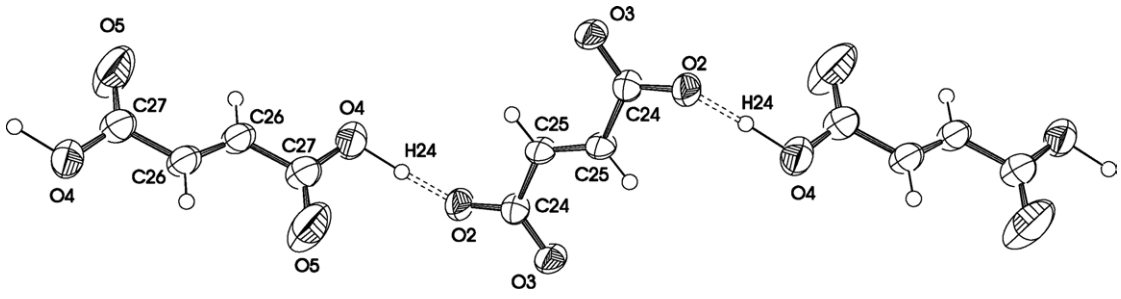

Fig. 8. The infinite chains formed by fumaric acid molecules (50% probability level ellipsoids) through hydrogen bonding.

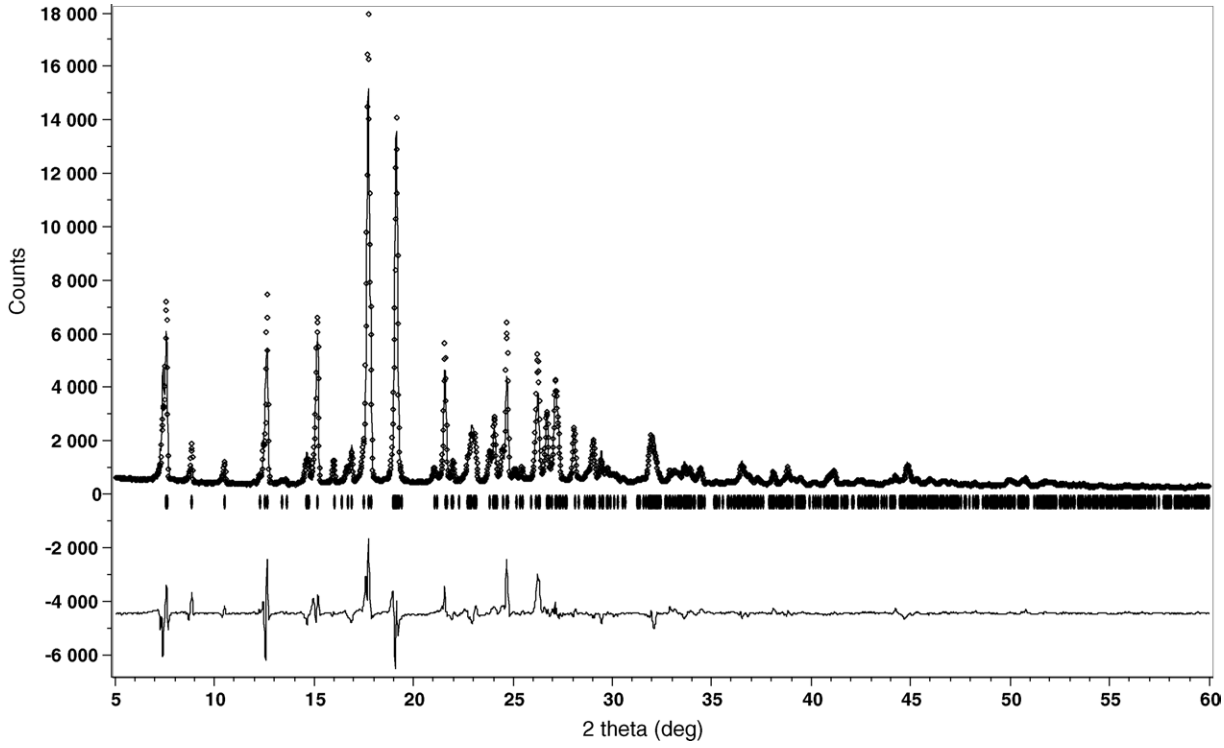

Fig. 9. The experimental X-ray powder pattern (λ = 1.5418 Å) of compound **1** (data points) and the calculated diagram from Rietveld refinement (single line). Line at the bottom represents the difference between experimental and calculated diffractograms. Positions of individual reflections are indicated by markers.

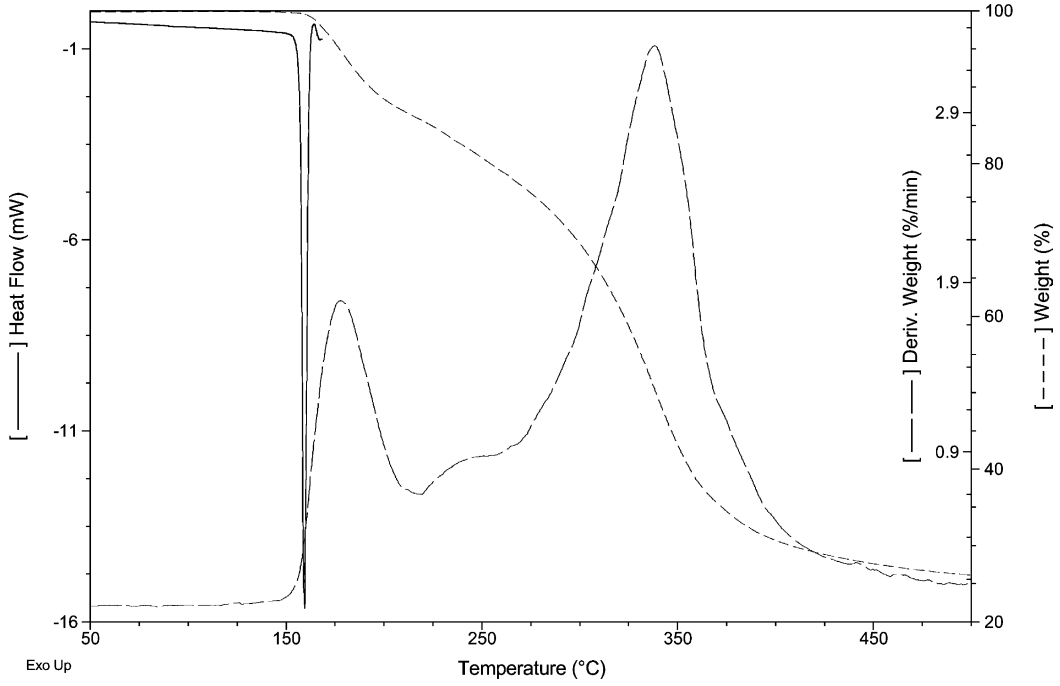

Fig. 10. DSC, TG and DTG profiles of **1**.

Table 2
Atomic coordinates ($\times 10^4$) and equivalent isotropic displacement parameters ($Å^2 \times 10^3$)

Atom	x	y	z	U_{eq}
Cl	−6808(2)	3672(1)	10771(1)	83(1)
F_1	−6101(4)	4951(3)	12209(3)	94(1)
F_2	2239(3)	3137(2)	7360(2)	58(1)
O_1	−318(5)	1535(4)	11762(3)	113(2)
O_2	2956(3)	7023(3)	3896(3)	50(1)
O_3	2050(3)	5338(2)	4836(3)	49(1)
O_4	4543(4)	8615(3)	2415(3)	63(1)
O_5	3433(7)	8304(4)	1073(3)	139(2)
C_1	−4824(8)	4339(4)	11891(4)	62(2)
C_2	−4975(6)	3706(4)	11199(4)	54(1)
C_3	−3659(6)	3100(4)	10843(4)	53(1)
C_4	−2212(6)	3099(4)	11219(4)	52(1)
C_5	−2081(7)	3719(5)	11932(4)	66(2)
C_6	−3377(8)	4354(5)	12256(5)	72(2)
C_7	−805(6)	2342(5)	10966(5)	65(2)
N_8	−90(5)	2553(3)	9923(3)	54(1)
C_9	−295(6)	3627(4)	8989(4)	54(1)
C_{10}	−512(5)	3410(4)	7895(4)	45(1)
C_{11}	794(5)	2573(3)	7597(4)	43(1)
C_{12}	994(6)	1508(4)	8619(4)	51(1)
C_{13}	1220(6)	1778(4)	9674(4)	60(1)
C_{14}	626(5)	2262(3)	6559(4)	41(1)
N_{15}	625(5)	3267(3)	5504(3)	40(1)
C_{16}	679(6)	2951(4)	4450(4)	51(1)
C_{17}	2197(6)	2295(4)	4202(4)	46(1)
N_{18}	3468(5)	2498(3)	4585(3)	53(1)
C_{19}	4840(6)	1925(4)	4355(4)	63(2)
C_{20}	5013(8)	1181(5)	3734(5)	70(2)
C_{21}	3672(10)	1002(5)	3359(5)	87(2)
C_{22}	2253(8)	1563(5)	3588(5)	75(2)
C_{23}	6588(8)	573(5)	3523(5)	109(3)
C_{24}	3168(5)	5978(4)	4450(4)	37(1)
C_{25}	4815(5)	5517(3)	4679(3)	36(1)
C_{26}	5020(5)	9851(4)	551(3)	48(1)
C_{27}	4258(6)	8840(4)	1374(5)	52(1)

U_{eq} is defined as one-third of the trace of the orthogonalized Uij tensor.

Table 3
Selected inter-atomic distances (Å), bond angles and torsion dihedral angles (°)

N_{15}—O_3	2.786(5)	O_1—C_7—N_8	121.0(5)
N_{15}—H_{15B}	0.81(4)	O_1—C_7—C_4	118.6(5)
N_{15}—H_{15B}—O_3	141(4)	N_8—C_7—C_4	120.4(4)
N_{15}—O_3[a]	2.695(5)	C_7—N_8—C_{13}	119.9(4)
N_{15}—H_{15A}	1.04(5)	C_7—N_8—C_9	125.2(4)
N_{15}—H_{15A}—O_3[a]	159(4)	C_{13}—N_8—C_9	114.0(4)
O_2—O_4	2.578(4)	F_2—C_{11}—C_{14}	106.3(3)
O_4—H_{24}	1.22(7)	F_2—C_{11}—C_{12}	106.8(4)
O_2—H_{24}	1.36(7)	C_{14}—C_{11}—C_{12}	110.9(4)
O_2—H_{24}—O_4	177(5)	F_2—C_{11}—C_{10}	106.1(3)
		C_{16}—N_{15}—C_{14}	113.3(4)
O_2—C_{24}	1.257(5)		
O_3—C_{24}	1.248(5)	C_{13}—N_8—C_7—O_1	4.9(9)
C_{27}—O_5	1.190(6)	C_{27}—O_4—O_2—C_{24}	100.8(5)
C_{27}—O_4	1.287(6)		

[a] Symmetry operation $-x, 1-y, 1-z$.

C_{13}, C_7 of the tertiary amine, and oxygen atom O_1 are located in a same plane (mean deviation of 0.072). The F_2 fluorine atom is found attached at the axial position to the cyclohexane-like cycle (N_8, C_9–C_{13}) with chair conformation. As represented in Fig. 7, the hydrogen atoms on nitrogen N_{15} are involved in bent medium strength hydrogen bonding with fumaric acid molecules (distances N_{15}—O_3 are 2.695 and 2.786 Å). Furthermore, as represented in Figs. 7 and 8, hydrogen bonding also occurs between neighbouring fumaric acid molecules. Through linear hydrogen bonding involving atoms O_2 and O_4 separated by 2.578 Å, fumaric acid molecules form infinite chains interacting (N_{15}—O_3 hydrogen bonds) with the protonated molecule $C_{20}H_{23}F_2N_3OCl^+$. Owing to the conjugated action of nitrogen basic centers on one of the fumaric acid molecules (see above the description of the N_{15}—O_3 hydrogen bond), the linear $O_2 \cdots H_{24}$—O_4 (angle O_2—H_{24}—O_4 of 177(5)°) hydrogen bond is asymmetric with O_4—H_{24} and O_2—H_{24} distances of 1.22(7) and 1.36(7) Å. The remaining oxygen atom O_5 of fumaric acid which is not involved in hydrogen bonding displays a larger atomic displacement parameter. Same feature is also found for the terminal methyl group (atom C_{23}) of the methylpyridin cycle.

The X-ray powder pattern was initially recorded (standard acquisition times and 2.5–30° theta domain) for identification purpose and polymorphism checking. The diffractogram is characteristic of a single phase with all diffraction lines indexing in the triclinic cell. Profile refinement led to refined parameters $a = 8.546(7)$ Å, $b = 12.402(5)$ Å, $c = 12.480(4)$ Å, $\alpha = 70.86(4)°$, $\beta = 82.09(5)°$, $\gamma = 83.58(5)°$. Fairly good Rietveld agreement factors, $R_{Bragg} = 7.88\%$ and $R_p = 9.80\%$, are obtained with the atomic positions and displacement parameters from X-ray single crystal structure determination. These values exclude the presence of any other polymorph in the sample. The experimental and calculated X-ray powder patterns ($\lambda = 1.5418$ Å) are represented in Fig. 9.

3.7. Thermal analysis and polymorph screening

The melting property and the thermal stability of **1** were investigated by DSC and TGA, respectively. DSC profile showed one only endothermic effect at 157 °C which corresponded to the melting of sample. The TG and DTG profiles (Fig. 10) indicated that the beginning of the mass loss occurred at the end of melting (1%, w/w at 165 °C). Two decomposition stages occurred after the melting with maximum kinetics at 183 and 346 °C, respectively. In our study conditions of polymorph screening, one only crystalline form of **1** was identified by DSC and XRPD. The melting property of this form was $T = 157$ °C and $\Delta H = 130$–140 J g^{-1}.

Acknowledgements

The authors wish to thank Prof. Hans J. Reich (University of Wisconsin, USA) with regard to computer software and are

grateful to Prof. A.D. Bain (McMaster University, Canada) for advice in chemical exchange line-shape analysis.

References

[1] B. Vacher, B. Bonnaud, P. Funes, N. Jubault, W. Koek, M.B. Assié, C. Cosi, J. Med. Chem. 41 (1998) 5070–5083.
[2] B. Vacher, B. Bonnaud, P. Funes, N. Jubault, W. Koek, M.B. Assié, C. Cosi, M. Kleven, J. Med. Chem. 42 (1999) 1648–1660.
[3] W. Koek, J.-F. Patoiseau, M.B. Assié, C. Cosi, M. Kleven, E. Dupont-Passelaigue, E. Carilla-Durand, J.-P. Valentin, G. John, J.P. Pauwels, J.-P. Tarayre, F.C. Colpaert, J. Pharmacol. Exp. Ther. 287 (1998) 266–283.
[4] F.C. Colpaert, J.-P. Tarayre, W. Koek, J.P. Pauwels, L. Bardin, X.J. Xu, Z. Wiesenfeld-Hallin, C. Cosi, E. Carilla-Durand, M.B. Assié, B. Vacher, Neuropharmacology 43 (2002) 945–958.
[5] B. Vacher, B. Bonnaud, W. Koek, Pyridin-2-yl-methylamine Derivatives, Method of Preparing and Application as Medicine, WO 98/22459, 1998.
[6] J.L. Maurel, B. Bonnaud, J.P. Ribet, B. Vacher, Procédé et intermédiaires de synthèse pour la préparation de dérivés de pyridin-2-yl-methylamine, FR 2820743–A1, 2001.
[7] H.J. Reich, WINDNMR, J. Chem. Educ. Software, 1996, 3D, 2.
[8] G.M. Sheldrick, SHELXL 97: A Program for Refining Crystal Structures, University of Göttingen, Germany, 1997.
[9] G.M. Sheldrick, SHELXS: A Program for Crystal Structures Solution, Vol. 97, University of Göttingen, Germany, 1997.
[10] G.M. Sheldrick, SHELX-76, Program for Crystal Structure Determination, University of Cambridge, Cambridge, 1976.
[11] L.J. Farrugia, J. Appl. Cryst. 30 (1997) 565.
[12] B.A. Hunter, C.J. Howard, LHPM—Rietica: A Computer Program for Rietveld Analysis of X-ray and Neutron Powder Diffraction Patterns, version 1.7.7, 1998, ANSTO, Lucas Heights Research Laboratories, Menai, Australia.
[13] E. Pretsch, T. Clerc, J. Seibl, W. Simon, Tables of Spectral Data for Structure Determination of Organic Compounds, Springer-Verlag, 1983.
[14] H.O. Kalinowski, S. Berger, S. Braun, Carbon-13 NMR Spectroscopy, John Wiley and Sons, 1988.
[15] H. Günther, NMR Spectroscopy, John Wiley and Sons, 1980.
[16] J. Jeener, B.H. Meier, P. Bachmann, R.R. Ernst, J. Chem. Phys. 71 (11) (1979) 4546–4553.
[17] M.H. Levitt, Spin Dynamics, John Wiley and Sons, 2001.
[18] K.C. Brown, R.L. Tyson, J.A. Weil, J. Chem. Educ. 75 (12) (1998) 1632–1635.
[19] A.D. Bain, Prog. Nucl. Magn. Reson. Spectrosc. 43 (2003) 63–103.